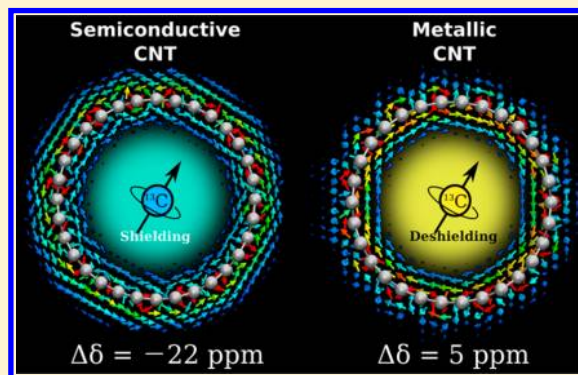


DFT Study on the NMR Chemical Shifts of Molecules Confined in Carbon Nanotubes

Pengju Ren,^{†,‡} Anmin Zheng,^{†,§} Xiulian Pan,[‡] Xiuwen Han,[‡] and Xinhe Bao^{*,‡}[†]State Key Laboratory of Catalysis, Dalian Institute of Chemical Physics, Chinese Academy of Sciences, Zhongshan Road 457, Dalian 116023, China[§]State Key Laboratory of Magnetic Resonance and Atomic and Molecular Physics, Wuhan Center for Magnetic Resonance, Wuhan Institute of Physics and Mathematics, Chinese Academy of Sciences, Wuhan 430071, China

ABSTRACT: Large magnetic shielding has been experimentally observed on certain organic molecules, regardless of their intrinsically different chemical natures, when they are confined within the carbon nanotubes. We investigated the underlying physics of the shielding effect by employing a series of density functional theory calculations on various molecule-confined-in-CNT systems. Particularly, the effects of the intermolecular interaction and the ring current of the CNTs on the chemical shifts of the confined molecules were investigated in detail. The results reveal that the changes in chemical shift mainly originate from the magnetic shielding induced by the delocalized π electrons. Electronic structure analysis for nonbonded interactions of host–guest and guest–guest indicated that this intermolecular interaction effect on chemical shift is significant for the polarizable molecules. Thus, the NMR responses of the molecules confined in CNTs are different from those of the molecules in other confining environments. Our study thus suggested that the chemical shift can be used as a probe to distinguish the molecules inside and outside of the CNT channels, as well as the type of CNTs (such as metallic and semiconducting).



1. INTRODUCTION

Certain physicochemical properties, including the molecular configuration, transport and phase transitions, of the molecules confined inside the nanoscale cavities or channels (carbon nanotubes, for example) were found to differ from their counterparts in the bulk.^{1–3} These confined systems have invoked extensive interest for potential applications in nanofluidic devices, gas sensors,⁴ catalysts,⁵ and drug delivery.⁶ Studies showed that the altered behavior and properties of the confined molecules originate from the unique structure of CNT's interior surface, which leads to the different host–guest interactions.^{7–9}

NMR spectroscopy has been ubiquitously employed to detect the local electronic structure and chemical environment of the probe nuclei.¹⁰ For example, the adsorption of water and xenon on the interior surface of the CNTs has been investigated using ¹H and ¹²⁹Xe NMR.^{11–14} In a recent study, we employed the ¹³C NMR to investigate the properties of several confined probe molecules, including the ¹³C-enriched benzene, the acetic acid (¹³CH₃COOH), and the methanol (¹³CH₃OH).^{15,16} The chemical shifts of all these confined molecules have remarkably decreased, regardless of their intrinsically different chemical natures. However, the decrement in the chemical shift varies when different CNT structures (i.e., single-walled CNTs, double-walled CNTs and multiwalled CNTs) were used. Our experiments provided the vivid evidence on the effect of CNT on the chemical shifts of the

molecules. The underlying microscopic physics, however, require further investigations.

DFT calculation can provide an important contribution for understanding the experimentally observed chemical shifts, thus has been used extensively to model the NMR signals. Besley et al. demonstrated that the chemical shifts of molecules can be affected by the confinement of the CNTs.¹⁷ Sebastiani et al. investigated the magnetic shielding of various types of CNTs.¹⁸ Kibalchenko et al. studied the NMR behavior of confined small molecules such as HCl and focused on the influence of magnetic shielding by the CNTs.¹⁹ In this work, we carried out a systematic investigation on the NMR response of a series of molecules confined within CNTs. We elaborated the effects of the external magnetic fields, the guest molecule–host CNT interactions and their relationships with the intrinsic electronic structures of CNTs. Three molecules (methanol, benzene, and acetic acid) with significantly different chemical natures were investigated. Our analysis revealed that strong magnetic shielding is induced by the delocalized π electrons of CNTs, which causes the significant chemical shift changes in different nanotubes.

Received: August 31, 2013

Revised: October 7, 2013

Published: October 9, 2013

2. METHODS AND COMPUTATIONAL DETAILS

All calculations were performed with Quantum ESPRESSO suite.²⁰ The geometries for the CNT (15, 0) and (16, 0) were taken directly from Zurek et al. first-principles optimized structures.²¹ Radius and calculated band gaps of CNTs are listed in Table 1. The adsorbents/nanotubes system are

Table 1. Radius and Band Gaps for CNTs Used in This Work

CNT	radius/nm	band gap/eV	
		this work	ref 21
(15, 0)	0.59	0.026	0.025
(16, 0)	0.63	0.53	0.531

modeled in a $1 \times 1 \times 2$ tetragonal supercell with lattice parameters $a = b = 16.0$ Å. In order to take van der Waals interactions into account, the recently developed dispersion interaction corrected DFT (DFT-D) method²² was introduced in the structure optimization. During the optimization, the structures of carbon nanotubes were fixed. The optimization convergence criterions are 1×10^{-4} Ry for energy and 1×10^{-3} Ry/Bohr for force.

Our calculations were carried out using ultrasoft pseudopotentials with the PBE exchange-correlation functional²³ and a plane-wave basis set. The plane-wave energy cutoff was set to 37 Ry for structures optimization and 42 Ry for NMR calculations. The k -point grid was set to $1 \times 1 \times 4$ for structures optimization by using the Monkhorst-Pack sampling method. Simulated NMR parameters for the CNTs systems are very sensitive to their band structures and k -point samplings. As for the semiconducting CNT (16, 0), the k -point grid was set to $1 \times 1 \times 14$, while for the metallic CNT (15, 0), the k -point grid was set to $1 \times 1 \times 40$. All parameters were tested for convergence.

To investigate the nonbonded interactions between adsorbents and the CNTs, we took the reduced density gradient (RDG) approach developed by Johnson et al.²⁴ The RDG is defined as

$$\text{RDG} = \frac{1}{2(3\pi^2)^{1/3}} \frac{|\nabla\rho|}{\rho^{4/3}}$$

where ρ is the electron density. In general, the RDG isosurface is set between 0.3 and 0.6 to visualize noncovalent interactions. All of the isovalues of RDG were set to 0.5 a.u. in this paper.

The value of $\Omega = \text{sign}(\lambda_2) \times \rho$ was defined to identify the type of nonbonded interactions, where λ_2 is the second eigenvalue of the electron-density Hessian (second derivative) matrix. Large negative values of Ω indicate the strong noncovalent interactions such as dipole–dipole or hydrogen bonding interactions. A Ω value near zero indicates the weak dispersion interaction (van der Waals interaction). Large and positive Ω values indicate the steric effects.

Chemical shifts and induced current tensors were calculated for each system using the gauge including projector augmented wave (GIPAW) approach.²⁵ The GIPAW approach has been successfully applied to investigate the NMR parameters of various condensed materials, such as zeolites and graphene-based structures.^{19,26} The application of a uniform external magnetic field \mathbf{B}_0 to atoms and molecules induces an inhomogeneous electron current density $\mathbf{J}_{\text{in}}(\mathbf{r})$. The $\mathbf{J}_{\text{in}}(\mathbf{r})$ is evaluated from the linear response to the perturbation due to the presence of \mathbf{B}_0 . The induced current maps shown in Figure 3a,b are the current of pseudised valence electrons and produced by axial direction (z direction) external field. The induced field $\mathbf{B}_{\text{in}}(\mathbf{r})$ tensor is calculated from the induced current using the Biot-Savart Law:

$$\mathbf{B}_{\text{in}}(\mathbf{r}) = \frac{1}{c} \int d\mathbf{r}' \mathbf{j}_{\text{in}}(\mathbf{r}') \times \frac{\mathbf{r}' - \mathbf{r}}{|\mathbf{r}' - \mathbf{r}|^3}$$

where c is the speed of light in atomic unit. For periodic systems, the Biot-Savart Law is applied in reciprocal space as

$$\tilde{\mathbf{B}}_{\text{in}}(\mathbf{G} \neq 0) = i \frac{4\pi}{c} \frac{\mathbf{G}}{|\mathbf{G}|^2} \times \mathbf{J}_{\text{in}}(\mathbf{G})$$

for $\mathbf{G} \neq 0$ components. The $\mathbf{G} = 0$ component for $\tilde{\mathbf{B}}_{\text{in}}$ is calculated separately by

$$\tilde{\mathbf{B}}_{\text{in}}(\mathbf{G} = 0) = 4\pi\alpha_{\chi_v} \cdot \mathbf{B}_0$$

where α is a diagonal tensor that depends on the macroscopic shape, χ_v is the magnetic volume susceptibility tensor. For CNT with a cylindrical shape, we choose $\alpha_{xx} = \alpha_{yy} = 1/2$ and $\alpha_{zz} = 2/3$, where the tube axis along the z direction. This choice was previously shown to yield the fastest convergence with respect to the intertube spacing.⁶ The chemical shift change induced by a magnetic field ($\Delta\delta_{\text{induce}}$) was calculated using the negative value of isotropic shielding constants σ_{iso} at the same position of the molecule for empty nanotube. σ_{iso} was calculated from the diagonalized symmetric part of the magnetic shielding tensor $\sigma(\mathbf{r})$:

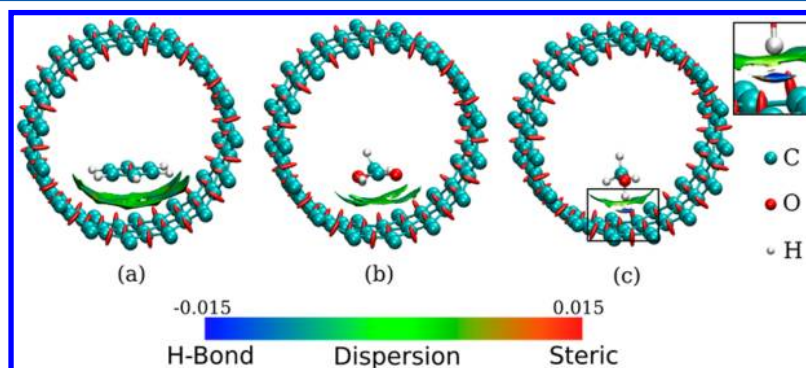
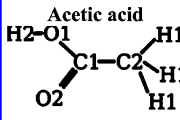
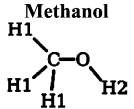


Figure 1. RDG isosurface (isovalue = 0.5 a.u.) of optimized structures for benzene (a), acetic acid (b), and methanol (c) inside CNT (15, 0). The mapping colors were defined with respect to the Ω values. The red areas indicate the steric effect, the green areas indicate the dispersion interactions, and the blue ones indicate the strong attractive interactions (e.g., hydrogen bond).

Table 2. Distances of Adsorbents from the CNT Wall (d), Chemical Shift Change ($\Delta\delta$), and the Corresponding Chemical Shift Change Caused by the Induced Magnetic Field ($\Delta\delta_{\text{induce}}$)

Molecule/CNT		(15,0)			(16,0)		
		$d/\text{\AA}$	$\Delta\delta/\text{ppm}$	$\Delta\delta_{\text{induce}}/\text{ppm}$	$d/\text{\AA}$	$\Delta\delta/\text{ppm}$	$\Delta\delta_{\text{induce}}/\text{ppm}$
Benzene	C	3.388	5.64	5.07	3.446	-22.45	-22.55
	H	3.013	5.22	5.05	3.110	-22.48	-22.54
 Acetic acid	C1	3.458	6.24	5.07	3.488	-21.53	-22.56
	C2	3.474	5.96	5.07	3.455	-22.22	-22.57
	O1	3.195	8.06	5.09	3.553	-22.65	-22.59
	O2	3.226	2.31	5.07	3.087	-26.68	-22.45
	H1	3.388	5.29	5.10	3.342	-22.45	-22.54
	H2	3.218	5.33	5.07	3.594	-22.36	-22.56
	H1	3.388	5.29	5.10	3.342	-22.45	-22.54
 Methanol	C	3.430	7.02	5.08	3.578	-21.67	-22.58
	O	3.287	12.11	5.07	3.470	-16.13	-22.56
	H1	3.399	5.12	5.10	3.546	-22.44	-22.57
	H2	2.332	6.57	5.08	2.520	-21.60	-22.54

$$\Delta\delta_{\text{induce}} = -\sigma_{\text{iso}}(\mathbf{r}) = -\frac{1}{3}\text{Tr}[\sigma(\mathbf{r})]$$

where shielding tensor $\sigma(\mathbf{r})$ can be obtained from

$$\sigma(\mathbf{r}) = -\frac{\mathbf{B}_{\text{in}}(\mathbf{r})}{\mathbf{B}_0}$$

All visualizations were done by using VMD,⁷ mayavi2,⁸ and Gnuplot.

3. RESULTS AND DISCUSSIONS

3.1. Structures and Interaction of Molecules with the Nanotube Wall. We first took CNT (15, 0) as a representative model system of the metallic tubes. An infinite periodic model was used because CNTs in experiments usually have an aspect ratio far larger than 100. We first examined the interactions of different molecules with the curved CNT walls. The optimized structures of the molecules adsorbed inside CNT (15, 0) are shown in Figure 1. Benzene tends to align its molecular plane parallel to the tube axis and close to the nanotube wall. Acetic acid is oriented with its C–C bond parallel to the tube axis. The most stable configuration of methanol adsorbed in CNTs has its hydroxyl group pointing toward the π electron cloud of CNTs. The centers of all adsorbent molecules are located at a distance of about 3.5 Å from the tube wall, which indicates that a weak noncovalent interaction dominates the host–guest interaction between the confined molecules and the CNT skeleton. The noncovalent interactions can be intuitively visualized by the RDG isosurfaces in real space, as shown in Figure 1. The red areas at the center of each six-member rings of the CNT wall, as well as on the benzene ring, are the typical indicators for the overlapping nonbonded electron clouds. In the case of benzene, there is a large green area between benzene and inner wall of CNT, which represents the π -stacking.²⁷ For acetic acid, a green region is observed between adsorbents and CNT, which is the result of van der Waals (vdW) dispersion interaction. For methanol, the blue area between the hydroxyl group of methanol and CNT indicates a hydrogen bond interaction with the π -acceptors.²⁸ In addition, the green area between the

methyl group of methanol and the CNT wall resembles the area of that of acetic acid.

3.2. Chemical Shifts of Adsorbed Molecules inside CNTs. With the GIPAW method we calculated the ^{13}C chemical shift of the adsorbed molecules inside the CNTs. $\Delta\delta$ is defined as the chemical shift difference of the confined molecules with respect to their isolated counterparts:

$$\Delta\delta = \delta_{\text{inCNT}} - \delta_{\text{isolated}}$$

which reflects the confinement effect on the adsorbed molecules. As listed in Table 2, all three molecules were predicted to have a deshielding for ^{13}C when they are adsorbed inside CNTs. For instance, $\Delta\delta$ for ^{13}C of benzene, acetic acid (methyl group), and methanol inside CNT (15, 0) is about +5.64, +5.96, and +7.02 ppm, indicating that $\Delta\delta$ is not sensitive to the specific molecule. A similar phenomenon was observed for $\Delta\delta$ of ^1H . In contrast, $\Delta\delta$ of ^{17}O depends on the specific molecules.

The difference of $\Delta\delta$ is likely related to the intermolecular interaction of confined molecules with the CNTs. It was demonstrated that the electronic structure of CNT has a remarkable effect on its electric, optical and magnetic properties.^{21,29} Therefore, we further studied the CNT (16, 0), which has a similar radius to CNT (15, 0) but a quite different electron structure. Interestingly, there is the magnetic shielding of about –22 ppm inside CNT (16, 0), as shown in Table 2. It is also not sensitive to the specific type of molecules. Therefore, $\Delta\delta$ is related to the intrinsic electronic structures of CNTs in magnetic fields, which has influenced the behavior and properties of confined molecules. Besley et al also observed that the chemical shifts of confined molecules are more sensitive to the type of CNTs rather than molecules.¹⁷

Molecules may be attached to the CNT surface with different relative orientations. We thus calculated the $\Delta\delta$ values as a function of the distances of atoms to the CNT wall. For example, within CNT (16, 0), two types of benzene configurations are considered: the one with benzene molecular plane parallel to the tube axis (Figure 2a) and the one with the plane perpendicular to the tube axis (Figure 2b). Table 3 shows that from the nanotube center ($y = 0$) to $y = 2.5$ Å, $\Delta\delta$ does not change. With the further increasing distance, $\Delta\delta$ varies with y .

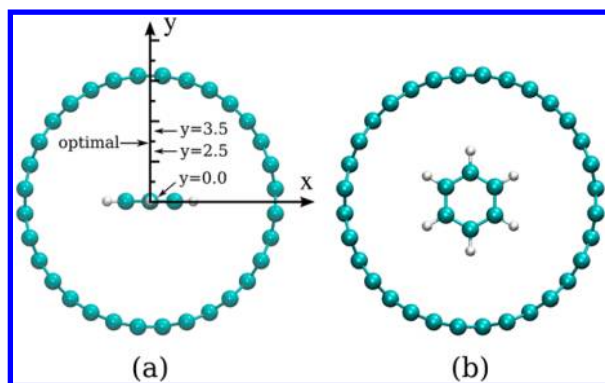


Figure 2. Configurations of benzene inside CNT (16, 0): (a) configuration with the molecular plane parallel to the tube axis (z axis) and y representing the distance of the atom to the CNT center; (b) configuration with the molecular plane perpendicular to the tube axis.

Table 3. Chemical Shift Changes ($\Delta\delta$) of Benzene in CNT (16, 0) as a Function with Different Configurations in Figure 2

configuration		$\Delta\delta$	
		^{13}C	^1H
(a)	y = 0.0	−22.35	−22.59
	y = 2.5	−22.35	−22.57
	y = 3.5	−23.22	−21.75
	optimal	−22.45	−22.48
(b)		−22.72	−22.95

However, the differences of $\Delta\delta$ are less than 1 ppm for all configurations, which indicates that the location of molecules within the CNT has only a small influence on the chemical shift.

3.3. Chemical Shifts Influenced by the Ring Current of CNTs. It is well-known that the NMR chemical shift reflects the chemical environment of the investigated nucleus, such as covalent bonding, functional groups, and nonbonding interaction. Particularly, a ring current appears in the aromatic molecules such as benzene and naphthalene under magnetic fields due to their delocalized π electrons. This, in turn, induces the magnetic shielding/deshielding, which can significantly affect the chemical shift of the nucleus.³⁰ For example, the ^3He nucleus is profoundly shielded by the ring current of the fullerene cage, which creates a chemical shift of −6.3 ppm.³¹ The CNTs can be envisioned as a large aromatic molecule. Sebastiani and Kibalchenko observed that the delocalized π electrons of CNTs can induce very strong magnetic shielding inside the CNTs.^{18,19} Therefore, one can expect that the induced magnetic shielding/deshielding effect will significantly affect the chemical shifts of molecules around them. We defined $\Delta\delta_{\text{induce}}$ as the chemical shift change (with respect to the isolated molecules) caused by the induced ring current. Table 2 demonstrates that the induced magnetic field has a significant influence on the chemical shift of molecules within CNTs. $\Delta\delta_{\text{induce}}$ is close to the corresponding $\Delta\delta$ particularly for ^1H and ^{13}C in both types of CNTs. This indicates that the NMR chemical shifts of ^1H and ^{13}C nuclei are mainly contributed from the induced magnetic shielding because of the delocalized π electrons of CNTs. Therefore, the significantly different $\Delta\delta$ within CNT (15, 0) and (16, 0) should be related to their different electronic structures, which is validated by the following computation on the spatial distributions of induced

ring current and magnetic shielding in both nanotubes (Figure 3).

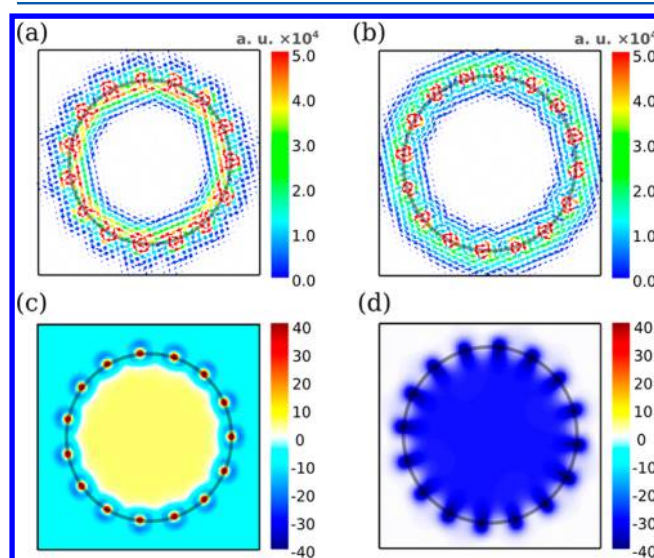


Figure 3. Induced ring current (a, b) and induced magnetic shielding distribution maps (c, d) for CNT (15, 0; a, c) and CNT (16, 0; b, d). The gray lines represent the CNT backbone. The induced current displayed here is that caused by the external field along the tube axis.

Applying a uniform external magnetic field \mathbf{B}_0 onto an aromatic molecule induces an inhomogeneous electron current density $\mathbf{J}_{\text{in}}(\mathbf{r})$, which in turn produces an induced magnetic field \mathbf{B}_{in} in the system. Figure 3a,b shows that the induced current flows along the whole carbon backbone which indicates the delocalized π electrons of CNTs. However, the distribution of the ring current is significantly different between (15, 0) and (16, 0). The inner ring current is more intense than the outer one for CNT (15, 0), whereas (16, 0) follows an opposite trend. This leads to a very different magnetic response. Figure 3c,d demonstrates different magnetic shielding distributions inside and outside of both types of CNTs. Consequently, molecules confined within (15, 0) and (16, 0) give different $\Delta\delta_{\text{induce}}$ as we have predicted in Table 2. Compared to the deshielding effect within metallic tube (15, 0; Figure 3c), the semiconducting tube (16, 0; Figure 3d) exhibits more significant shielding effect inside the tube. Figure 3c,d also demonstrates that the magnetic shielding is homogeneously distributed inside both nanotubes, except the region very close to the nanotube wall (e.g., <2 Å to the wall). Therefore, it is understandable that the resulting $\Delta\delta$ is almost independent of their relative location with respect to the CNT wall, as illustrated in Table 3. An interesting observation is that the induced magnetic shielding distribution outside of the CNT is clearly different from that inside the CNT. For example, the induced magnetic shielding value decays to zero rapidly outside of the semiconducting tube (16, 0). Consequently, molecules adsorbed on the outer wall of this nanotube exhibit no change in the chemical shift, namely, $\Delta\delta = 0$. In contrast, the magnetic shielding outside of metallic CNT (15, 0) decays very slowly. Furthermore, the sign of induced magnetic shielding outside is opposite to that inside metallic CNT (15, 0), which results in magnetic shielding for molecules adsorbed on outside of this tube.

3.4. Chemical Shifts Influenced by the Guest–Host and the Guest–Guest Interactions. Compared with ^1H and

^{13}C , $\Delta\delta_{\text{induce}}$ for ^{17}O in methanol and acetic acid differs from the corresponding total chemical shift changes ($\Delta\delta$) by about 3–7 ppm. The different responses of ^1H , ^{13}C , and ^{17}O nuclei can be explained by their different intermolecular interactions with CNTs. Kibalchenko discovered that the interaction effect is significant when the radius of CNTs is small.¹⁹ In this study, the chemical shift changes of ^1H and ^{17}O in hydroxyl group are found to be quite different from its $\Delta\delta_{\text{induce}}$ (1.5 ppm for ^1H , 7 ppm for ^{17}O), even though the nanotubes are pretty large. Although these molecules interact with the CNT walls mainly through van der Waals interaction and hydrogen bonding, as illustrated by Figure 1, CNTs possess a large polarizability of π electron cloud,³² which influences the electronic environment around the probe nucleus through the dipole–induced dipole interaction.³³ This can be seen from the calculated charge density change ($\Delta\rho$) of each molecule adsorbed inside CNT (15, 0; Figure 4), where $\Delta\rho$ is defined as $\Delta\rho = \rho(\text{total}) -$

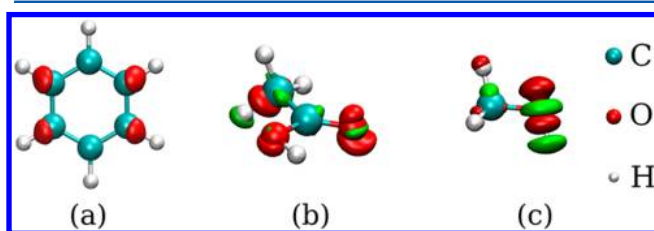


Figure 4. Differential charge density isosurface (isoval = 0.0004 bohr⁻³) for benzene (a), acetic acid (b), and methanol (c) inside CNT (15, 0). The red regions indicate electron accumulation and the green regions indicate electron depletion. The parts of isosurface on carbon nanotube are not shown.

$\rho(\text{CNT}) - \rho(\text{molecule})$. $\Delta\rho$ of the hydrophobic methyl group has a very tiny change, which indicates a weak interaction of hydrophobic methyl groups with the CNT. This validates the conclusion in the previous section that $\Delta\delta$ of carbon and hydrogen in the methyl group is mainly contributed by the $\Delta\delta_{\text{induce}}$ (Table 2). In contrast, an obvious change in the charge density of oxygen atom is observed for methanol, which indicates the formation of the induced dipole. This causes an approximate 3–7 ppm shift for ^{17}O in methanol and acetic acid.

Besides the host–guest interaction, the interaction between guest molecules can influence the chemical shifts as well. By combining the first principle molecule dynamics and GIPAW approach, Huang Patrick et al showed that the ^1H chemical shifts of water confined in the CNT vary in a range up to more than 10 ppm, which is due to the hydrogen bonding network and the variety of local environment.³⁴ Therefore, we took a methanol dimer encapsulated in the CNT as the model to investigate this effect on the chemical shift. The structure of the methanol dimer in CNT (16, 0) is presented in Figure 5. According to RDG isosurface (Figure 5a), a relatively strong hydrogen bond is formed between these two methanol molecules, where methanol A is the hydrogen bond donor and B is the acceptor. Table 4 shows that the hydrogen bonding between methanol molecules results in the significantly shift of $\Delta\delta$ for hydroxylic ^1H and ^{17}O , about 5 ppm shift for ^1H and 10 ppm for ^{17}O in contrast to $\Delta\delta_{\text{induce}}$ (–22 ppm). In comparison, a maximum shift of 2 ppm was predicted for ^{13}C in methanol B. This is also confirmed by the change of charge density ($\Delta\rho$) in Figure 5b.

3.5. Discussion. Current investigation gave a microscopic insight into the underlying physics of the chemical shifts of

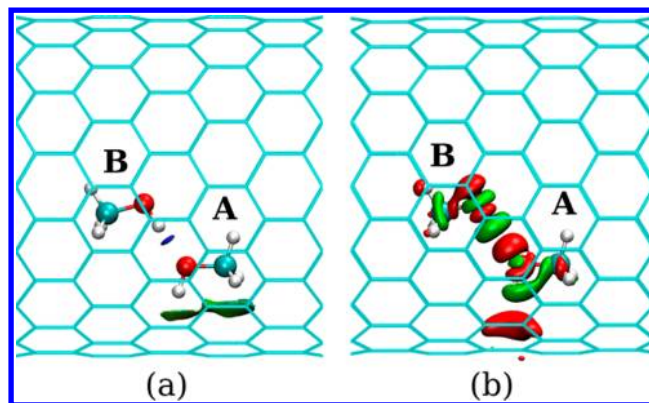


Figure 5. RDG isosurface (a) and $\Delta\rho$ isosurface (b) of a methanol dimer encapsulated in CNT (16, 0). The color scale of RDG is same to Figure 1. The isovalue of $\Delta\rho$ is 0.001 bohr⁻³.

Table 4. Chemical Shift Changes ($\Delta\delta$) of a Methanol Dimer in CNT (16, 0)

structure	$\Delta\delta$			
	^{13}C	$^1\text{H}(\text{C})$	$^1\text{H}(\text{O})$	^{17}O
A	–22.31	–22.39	–20.24	–12.08
B	–24.29	–22.56	–17.85	–24.04

molecules confined inside the CNT channels. The chemical shift is controlled by two main factors: ring current and intermolecular interaction. Calculations revealed that $\Delta\delta$ is mainly determined by the ring current of CNTs, as also suggested by Besley¹⁷ and Kibalchenko.¹⁹ The similar $\Delta\delta_{\text{induce}}$ for three molecules with different chemical natures indicate that the influence of the host–guest interaction on the ring current is much smaller. On the other hand, the change in the electronic structure (as demonstrated by Figures 4 and 5) induced by the host–guest and guest–guest interactions may also affect the NMR parameters of the molecules (especially for the polarizable atoms, such as ^{17}O in methanol) confined in CNTs. Due to the π -hydrogen bond interaction between methanol and CNTs, the chemical shift changes ($\Delta\delta$) of ^1H and ^{17}O in hydroxyl group are quite different from $\Delta\delta_{\text{induce}}$. The calculation of a methanol dimer in a CNT suggested that the intermolecular interaction may also significantly affect the chemical shift. Therefore, the chemical shift also depends on the amount of adsorbents and their local structures in CNTs.

The chemical shifts for molecules confined in CNTs are obviously different from those confined within zeolites.^{35–37} For molecules within zeolite pores, the chemical shift change mainly originates from the guest–host and guest–guest noncovalent interactions. As shown in our previous study, a highly overlapping distribution of electron clouds in the confined environment through van der Waals interactions is present, which will affect not only the adsorption configurations, but also the NMR properties for molecules confined in the micropores of zeolites.³⁷ In contrast, CNTs exhibit a unique graphitic structure, which leads to an induced magnetic field in addition to the guest–host and guest–guest interactions concomitant with the one-dimensional nanochannel. There are several distinctive characters for the chemical shift in the CNT confinement environment with comparison with other confined systems. First, $\Delta\delta_{\text{induce}}$ is the main factor for $\Delta\delta$ in CNTs, especially for molecules with small polarizability. $\Delta\delta_{\text{induce}}$ is element and molecule insensitive, which is unique. Second,

$\Delta\delta_{\text{induce}}$ does not depend on the location of molecules within CNTs. The effect of the host–guest interaction on the chemical shifts rapidly reduces with the interaction distance, whereas $\Delta\delta_{\text{induce}}$ is relatively homogeneous inside the CNTs. Finally, $\Delta\delta_{\text{induce}}$ is very sensitive to the structure of CNTs, particularly the electronic structures. Therefore, the chemical shift differs considerably for molecules confined inside metallic and semiconducting tubes.

Our investigation suggested that the molecules in a semiconducting nanotube exhibit a chemical shift distinctively different from those in a metallic tube. For example, benzene within CNT (15, 0) gives a shift by +5 and −22 ppm within CNT (16, 0). However, direct comparison with the experimental results is difficult so far because chemically synthesized CNTs usually contain CNTs with mixed diameters and chiralities. It still remains a challenge with currently available techniques to synthesize the high purity semiconducting and metallic nanotubes with a reasonable quantity for NMR experiments. Furthermore, the configuration of the adsorbents in CNTs, such as monomer or dimer for methanol, will also significantly influence the chemical shift. Nevertheless, the results here provide a new concept of distinguishing the molecules inside and outside of CNT channels, as well as metallic and semiconducting tubes in the future.

4. CONCLUSION

We carried out DFT calculations to unveil the mechanism of different experimentally observed chemical shifts for molecules confined within the CNT channels. By elaborating on the effects of the ring current, guest molecule–host CNT and guest–guest interactions, we found that the ring current caused by the delocalized π electrons of CNTs plays a critical role in the chemical shift. The vector map of ring current provides an intuitive and insight view to understand the effect of CNTs. This effect results in a similar shielding effect for all nuclei, for example, ^{13}C , ^1H , and ^{17}O in three different molecules. Electronic structure analysis for the host–guest and the guest–guest interactions indicates that the electronic effect makes the significant contribution to the chemical shifts of the polarizable atoms (such as ^{17}O). Therefore, the chemical shift in the CNTs confinement environment is quite different from other confined systems such as in zeolites. Furthermore, this magnetic shielding effect strongly depends on the electronic structure of CNTs, which provides another effective approach for distinguishing the metallic versus semiconducting character of the CNTs besides UV–vis absorption and Raman spectroscopies. The magnetic shielding differs significantly inside and outside of the CNT channel, which will enable experimental studies of molecule behavior and diffusion dynamics within CNT channels.

AUTHOR INFORMATION

Corresponding Author

*E-mail: xhbao@dicp.ac.cn.

Author Contributions

[†]These authors have contributed equally (P.R. and A.Z.).

Notes

The authors declare no competing financial interest.

ACKNOWLEDGMENTS

We thank Prof. Yining Huang from the University of Western Ontario and Prof. Wei Zhuang from Dalian Institute of

Chemical Physics for fruitful discussions. We acknowledge the financial support from the Natural Science Foundation of China (11079005, 21033009, and 21173215) and the Ministry of Science and Technology of China (2012CB224806 and 2009CB623507).

REFERENCES

- (1) Koga, K.; Gao, G. T.; Tanaka, H.; Zeng, X. C. Formation of Ordered Ice Nanotubes Inside Carbon Nanotubes. *Nature* **2001**, *412*, 802–805.
- (2) Hummer, G.; Rasaiah, J. C.; Noworyta, J. P. Water Conduction through the Hydrophobic Channel of a Carbon Nanotube. *Nature* **2001**, *414*, 188–190.
- (3) Urita, K.; Shiga, Y.; Fujimori, T.; Iiyama, T.; Hattori, Y.; Kanoh, H.; Ohba, T.; Tanaka, H.; Yudasaka, M.; Iijima, S.; et al. Confinement in Carbon Nanospace-Induced Production of KI Nanocrystals of High-Pressure Phase. *J. Am. Chem. Soc.* **2011**, *133*, 10344–10347.
- (4) Zhang, T.; Mubeen, S.; Myung, N. V.; Deshusses, M. A. Recent Progress in Carbon Nanotube-Based Gas Sensors. *Nanotechnology* **2008**, *19*, 332001.
- (5) Pan, X.; Bao, X. The Effects of Confinement Inside Carbon Nanotubes on Catalysis. *Acc. Chem. Res.* **2011**, *44*, 553–562.
- (6) Hilder, T. A.; Hill, J. M. Modeling the Loading and Unloading of Drugs into Nanotubes. *Small* **2009**, *5*, 300–308.
- (7) Guan, J.; Pan, X.; Liu, X.; Bao, X. Syngas Segregation Induced by Confinement in Carbon Nanotubes: A Combined First-Principles and Monte Carlo Study. *J. Phys. Chem. C* **2009**, *113*, 21687–21692.
- (8) Zoberbier, T.; Chamberlain, T. W.; Biskupek, J.; Kuganathan, N.; Eyhusen, S.; Bichoutskaia, E.; Kaiser, U.; Khlobystov, A. N. Interactions and Reactions of Transition Metal Clusters with the Interior of Single-Walled Carbon Nanotubes Imaged at the Atomic Scale. *J. Am. Chem. Soc.* **2012**, *134*, 3073–3079.
- (9) Yu, L.; Li, W.-X.; Pan, X.; Bao, X. In- and Out-Dependent Interactions of Iron with Carbon Nanotubes. *J. Phys. Chem. C* **2012**, *116*, 16461–16466.
- (10) Hunger, M.; Weitkamp, J. In Situ Magnetic Resonance Techniques: Nuclear Magnetic Resonance. In *In Situ Spectroscopy of Catalysts*; Weckhuysen, B. M., Ed.; American Scientific Publishers: Valencia, California, 2004; pp 177–218.
- (11) Chen, Q.; Herberg, J. L.; Mogilevsky, G.; Wang, H.-J.; Stadermann, M.; Holt, J. K.; Wu, Y. Identification of Endohedral Water in Single-Walled Carbon Nanotubes by ^1H NMR. *Nano Lett.* **2008**, *8*, 1902–1905.
- (12) Sekhaneh, W.; Kotecha, M.; Dettlaff-Weglikowska, U.; Veeman, W. S. High Resolution NMR of Water Absorbed in Single-Wall Carbon Nanotubes. *Chem. Phys. Lett.* **2006**, *428*, 143–147.
- (13) Kneller, J. M.; Soto, R. J.; Surber, S. E.; Colomer, J.-F.; Fonseca, A.; Van Tendeloo, G.; Pietraß, T. TEM and Laser-Polarized ^{129}Xe NMR Characterization of Oxidatively Purified Carbon Nanotubes. *J. Am. Chem. Soc.* **2000**, *122*, 10591–10597.
- (14) Romanenko, K. V.; Fonseca, A.; Dumonteil, S.; Nagy, J. B.; d'Espinoze de Lacaille, J.-B.; Lapina, O. B.; Fraissard, J. ^{129}Xe NMR Study of Xe Adsorption on Multiwall Carbon Nanotubes. *Solid State Nucl. Magn. Reson.* **2005**, *28*, 135–141.
- (15) Liu, X.; Pan, X.; Shen, W.; Ren, P.; Han, X.; Bao, X. NMR Study of Preferential Endohedral Adsorption of Methanol in Multiwalled Carbon Nanotubes. *J. Phys. Chem. C* **2012**, *116*, 7803–7809.
- (16) Zhang, H.; Pan, X.; Han, X.; Liu, X.; Wang, X.; Shen, W.; Bao, X. Enhancing Chemical Reactions in a Confined Hydrophobic Environment: An NMR Study of Benzene Hydroxylation in Carbon Nanotubes. *Chem. Sci.* **2013**, *4*, 1075–1078.
- (17) Besley, N. A.; Noble, A. NMR Chemical Shifts of Molecules Encapsulated in Single Walled Carbon Nanotubes. *J. Chem. Phys.* **2008**, *128*, 101102.
- (18) Sebastiani, D.; Kudin, K. N. Electronic Response Properties of Carbon Nanotubes in Magnetic Fields. *ACS Nano* **2008**, *2*, 661–668.

- (19) Kibalchenko, M.; Payne, M. C.; Yates, J. R. Magnetic Response of Single-Walled Carbon Nanotubes Induced by an External Magnetic Field. *ACS Nano* **2010**, *5*, 537–545.
- (20) Giannozzi, P.; Baroni, S.; Bonini, N.; Calandra, M.; Car, R.; Cavazzoni, C.; Ceresoli, D.; Chiarotti, G. L.; Cococcioni, M.; Dabo, I.; et al. QUANTUM ESPRESSO: A Modular and Open-Source Software Project for Quantum Simulations of Materials. *J. Phys.: Condens. Matter* **2009**, *21*, 395502.
- (21) Zurek, E.; Pickard, C. J.; Walczak, B.; Autschbach, J. Density Functional Study of the ^{13}C NMR Chemical Shifts in Small-to-Medium-Diameter Infinite Single-Walled Carbon Nanotubes. *J. Phys. Chem. A* **2006**, *110*, 11995–12004.
- (22) Grimme, S. Accurate Description of van der Waals Complexes by Density Functional Theory Including Empirical Corrections. *J. Comput. Chem.* **2004**, *25*, 1463–1473.
- (23) Perdew, J. P.; Burke, K.; Ernzerhof, M. Generalized Gradient Approximation Made Simple. *Phys. Rev. Lett.* **1996**, *77*, 3865.
- (24) Johnson, E. R.; Keinan, S.; Mori-Sánchez, P.; Contreras-García, J.; Cohen, A. J.; Yang, W. Revealing Noncovalent Interactions. *J. Am. Chem. Soc.* **2010**, *132*, 6498–6506.
- (25) Mauri, F.; Pfrommer, B. G.; Louie, S. G. Ab Initio Theory of NMR Chemical Shifts in Solids and Liquids. *Phys. Rev. Lett.* **1996**, *77*, 5300–5303.
- (26) Bonhomme, C.; Gervais, C.; Babonneau, F.; Coelho, C.; Pourpoint, F.; Azais, T.; Ashbrook, S. E.; Griffin, J. M.; Yates, J. R.; Mauri, F.; et al. First-Principles Calculation of NMR Parameters Using the Gauge Including Projector Augmented Wave Method: A Chemist's Point of View. *Chem. Rev.* **2012**, *112*, 5733–5779.
- (27) Tournus, F.; Latil, S.; Heggie, M. L.; Charlier, J.-C. π -stacking Interaction Between Carbon Nanotubes and Organic Molecules. *Phys. Rev. B* **2005**, *72*, 075431.
- (28) Suzuki, S.; Green, P. G.; Bumgarner, R. E.; Dasgupta, S.; Goddard, W. A.; Blake, G. A. Benzene Forms Hydrogen Bonds with Water. *Science* **1992**, *257*, 942–945.
- (29) Dresselhaus, M. S.; Dresselhaus, G.; Avouris, P. *Carbon Nanotubes: Synthesis, Structure, Properties, and Applications*; Springer: New York, 2001.
- (30) Chen, Z.; Wannere, C. S.; Corminboeuf, C.; Puchta, R.; Schleyer, P. von R. Nucleus-Independent Chemical Shifts (NICS) as an Aromaticity Criterion. *Chem. Rev.* **2005**, *105*, 3842–3888.
- (31) Saunders, M.; Jiménez-Vázquez, H. A.; Cross, R. J.; Mroczkowski, S.; Freedberg, D. I.; Anet, F. A. L. Probing the Interior of Fullerenes by ^3He NMR Spectroscopy of Endohedral $^3\text{He}@C_{60}$ and $^3\text{He}@C_{70}$. *Nature* **1994**, *367*, 256–258.
- (32) Lu, D.; Li, Y.; Rotkin, S. V.; Ravaioli, U.; Schulten, K. Finite-Size Effect and Wall Polarization in a Carbon Nanotube Channel. *Nano Lett.* **2004**, *4*, 2383–2387.
- (33) Kazachkin, D. V.; Nishimura, Y.; Witek, H. A.; Irle, S.; Borguet, E. Dramatic Reduction of IR Vibrational Cross Sections of Molecules Encapsulated in Carbon Nanotubes. *J. Am. Chem. Soc.* **2011**, *133*, 8191–8198.
- (34) Huang, P.; Schwegler, E.; Galli, G. Water Confined in Carbon Nanotubes: Magnetic Response and Proton Chemical Shieldings. *J. Phys. Chem. C* **2009**, *113*, 8696–8700.
- (35) Jameson, C. J. Xe Chemical Shift Tensor in Silicalite and SSZ-24. *J. Am. Chem. Soc.* **2004**, *126*, 10450–10456.
- (36) Bagno, A.; Saielli, G. Understanding the Extraordinary Deshielding of ^{129}Xe in a Permetallated Cryptophane by Relativistic DFT. *Chem.—Eur. J.* **2012**, *18*, 7341–7345.
- (37) Zheng, A.; Han, B.; Li, B.; Liu, S.-B.; Deng, F. Enhancement of Brønsted Acidity in Zeolitic Catalysts Due to an Intermolecular Solvent Effect in Confined Micropores. *Chem. Commun.* **2012**, *48*, 6936–6938.